Au–Cu Alloy nanoparticles confined in SBA-15 as a highly efficient catalyst for CO oxidation†

Xiaoyan Liu,[ab] Aiqin Wang,[a] Xiaodong Wang,[a] Chung-Yuan Mou[c] and Tao Zhang*[a]

Received (in Cambridge, UK) 13th March 2008, Accepted 7th April 2008
First published as an Advance Article on the web 2nd May 2008
DOI: 10.1039/b804362k

Au–Cu Alloy nanoparticles with sizes of ~3 nm were prepared in the confined space of SBA-15 and showed much better performance than monometallic particles in catalyzing CO oxidation even with the rich presence of H_2.

Gold had long been regarded as a very stable and catalytically inert metal until Haruta *et al*. found the surprisingly high activity of supported gold catalysts for low-temperature CO oxidation.[1] Since then, interest in gold catalysis has grown exponentially and gold catalysts have been applied to a variety of reactions,[2–8] among which CO oxidation is the most intensively studied.[9–14]

For CO oxidation on gold catalysts, oxygen adsorption and activation is regarded as a rate-limiting step. Since oxygen dissociation is inhibited on single gold crystals, it is believed to occur on the support or at the metal support interface.[10–12] The supports thus have been classified into active (TiO_2, Fe_2O_3) and inert (SiO_2) ones in terms of their capability to activate oxygen.[10] Therefore, to prepare a highly active gold catalyst on an inert support is rather difficult and it remains a significant challenge so far. Yan *et al*.[15] modified the support surface by decorating a thin layer of reducible metal oxides on the inert silica support to achieve an enhanced activity; Budroni and Corma[16] obtained a highly active gold catalyst on the silica support by improving the metal–support interaction through an elaborately designed synthesis route. Alternatively, one can alloy gold with a second metal on which oxygen can be adsorbed and activated easily. In our previous work,[17] we prepared a Au–Ag alloy catalyst by a one-pot synthesis route, and observed a strong synergy between gold and silver for CO oxidation. However, a major drawback associated with this one-pot method was the uncontrollable and relatively large particle sizes (20–30 nm), which led to loss of activity in the presence of H_2 and thus largely limited its application in a fuel-cell hydrogen purification system. It is therefore desirable to develop a new gold alloy system for obtaining a highly active and selective catalyst for CO oxidation even in a H_2-rich stream. Herein, we designed a new gold catalyst system, in which gold was alloyed with copper to obtain modified surface properties. Moreover, the gold–copper alloy particles were confined in the nanospace of SBA-15 to prevent their possible growth to large particles under a high-temperature treatment. The result showed that by alloying gold with copper, the particles became even smaller than pure gold, and they were highly dispersed and thermally stable. Such gold–copper alloy nanoparticles exhibited superior performance than the monometallic particles in catalyzing CO oxidation with or without the rich presence of H_2. To the best of our knowledge, this is the first report that very small and thermally stable Au–Cu alloy particles were obtained *via* a facile synthesis route and that gold and copper can synergetically catalyze the CO oxidation.

To prepare SBA-15 supported gold–copper alloy nanoparticles, the support surface was first functionalized with APTES ($H_2N(CH_2)_3Si(OEt)_3$) according to our previous report.[18] Then, a certain amount of tetrachloroaurate ($HAuCl_4$) solution was added to the APTES-SBA-15 followed by reduction with $NaBH_4$. After filtration and washing, the recovered solid was added to an aqueous solution of copper nitrate ($Cu(NO_3)_2{\cdot}3H_2O$) and again followed by reduction with $NaBH_4$. After filtration and washing for several times, the solid was dried at 110 °C, calcined at 500 °C in air for 6 h and reduced at 550 °C in H_2 for 2 h to obtain the Au–Cu/SBA-15 catalyst. In this synthesis, the reduction with $NaBH_4$ was proved to be crucial for obtaining the highly dispersed nanoparticles and the final reduction with H_2 was necessary for the formation of Au–Cu alloy. The amount of tetrachloroaurate and copper nitrate was varied to give the desired Au : Cu atomic ratios, and the nominal total metal loading was 6 wt%. The textural properties and the chemical compositions of the Au–Cu/SBA-15 are listed in Table 1.

Fig. 1 presents XRD patterns of the Au–Cu/SBA-15 samples with different Au : Cu atomic ratios. Au/SBA-15 shows four diffraction lines at 2θ = 38.2, 44.6, 64.7 and 77.5°, which can be indexed as Au(111), (200), (220) and (311) reflections.[17] Cu/SBA-15 presents only one diffraction peak at 2θ = 43.3° with very low intensity, which is characteristic of metallic Cu.[19] Different from either Au/SBA-15 or Cu/SBA-15, the two Au–Cu/SBA-15 samples show the diffraction lines positioned between Au/SBA-15 and Cu/SBA-15, and the peaks shift toward high angles with an increase in the Cu content. This result implies that Au–Cu alloy is formed. Moreover, compared with the Au/SBA-15, the two Au–Cu/SBA-15 samples give broader XRD peaks, suggesting that the Au–Cu alloy has a smaller particle size than the Au/SBA-15. According to the Sherrer equation, the Au–Cu alloy particle size is estimated to be 2.4 nm at Au : Cu = 3 : 1 and 2.8 nm at Au : Cu = 1 : 1, both of which are smaller than the gold particle size of 5.0 nm.

Fig. 2 shows the UV-Vis spectra of Au–Cu/SBA-15 as compared with those of the Au/SBA-15 and Cu/SBA-15. The Au/SBA-15 presents a single and strong absorption peak

[a] *State Key Laboratory of Catalysis, Dalian Institute of Chemical Physics, Chinese Academy of Sciences, PO Box 110, Dalian, 116023, PR China. E-mail: taozhang@dicp.ac.cn; Fax: +86-411-84691570; Tel: +86-411-84379015*
[b] *Graduate University of Chinese Academy of Sciences, Beijing, 100049, PR China*
[c] *Department of Chemistry, National Taiwan University, Taipei, 106, Taiwan*

† Electronic supplementary information (ESI) available: Details of catalyst preparation and characterization. See DOI: 10.1039/b804362k

Table 1 Textural parameters, chemical compositions and turnover frequencies (TOFs) of Au–Cu/SBA-15 for CO oxidation

Catalysts	Actual metal loading[a] (wt%)	Nominal Au/Cu (molar ratio)	Actual Au/Cu[a] (molar ratio)	S_{BET}/ $m^2\ g^{-1}$	D_{pore}/ nm	Particle size[b]/nm	Specific rate/ $mol_{CO}\ g_{Au}^{-1}\ h^{-1}$	Contact time/ $g_{cat}\ h\ mol_{CO}^{-1}$	TOF/s^{-1}
Au/SBA-15	6.0	1 : 0	1 : 0	568	6.7	5.6	0.08[c]	8.6[c]	0.02[c]
Au–Cu/SBA-15	4.8	3 : 1	2.26 : 1	535	7.0	2.9	0.32[c]	4.3[c]	0.04[c]
Au–Cu/SBA-15	4.1	1 : 1	0.99 : 1	525	7.0	3.0	0.43[c]	4.3[c]	0.06[c]
Au/MCM-41[d]	4.2	—	—	1010	2.2	4.2	—	—	0.02[e]
Au/SiO_2[f]	1.7	—	—	540	7.0	3.6	0.48[g]	93	—

[a] Determined by ICP. [b] Determined by TEM. [c] Obtained by controlling the CO conversion below 10% at 20 °C *via* diluting the catalyst with SiC, CO : O_2 : He = 1 : 1 : 98, GHSV = 240 000 (for Au/SBA-15) and 480 000 (for Au–Cu/SBA-15) ml $g_{cat}^{-1}\ h^{-1}$. The TOFs were calculated according to the relationship between the degree of dispersion and particle size proposed in ref. 9. [d] Prepared by CVD in ref. 20. [e] TOF at 273 K. [f] Ref. 16. [g] Specific rate at 30 °C.

at 514 nm due to the surface plasma resonance of gold nanoparticles, while the Cu/SBA-15 gives a very weak absorption peak at 579 nm. For the Au–Cu/SBA-15 samples, the surface plasma bands in the intermediate positions between those of the Au/SBA-15 and Cu/SBA-15 could be observed. Moreover, red shift occurred with the Au : Cu atomic ratio changing from 3 : 1 to 1 : 1. This result again suggests the formation of Au–Cu alloy.[19]

To visually observe the particle size distribution of the Au–Cu alloy, we performed transmission electron microscopy (TEM). As shown in Fig. 3, all the nanoparticles are uniformly distributed in the channels of SBA-15. Gold particles in the Au/SBA-15 have an average particle size of about 5.6 nm, while copper particles in the Cu/SBA-15 are in the range of 2–3 nm. Interestingly, upon alloying Au with Cu, the particle size becomes much smaller than that of gold, 2.9 nm for Au : Cu = 3 : 1 and 3.0 nm for Au : Cu = 1 : 1. Clearly, this is well consistent with the XRD result. Further examination on the Au–Cu(1/1)/SBA-15 with HRTEM reveals that the *d* spacing value in a single particle is about 2.23 Å, which is in good agreement with the value calculated from the XRD of the Au–Cu alloy. This again confirms that the particles are not a mixture of separate gold and copper particles, but composed of Au–Cu alloy. From the nitrogen adsorption–desorption, the average pore diameter (D_{pore}) of the Au–Cu/SBA-15 was calculated to be about 7 nm (Table 1), which was larger than the Au–Cu alloy particle size. Thus, the pores could not be blocked by the particles within them and the particles were therefore easy to be accessible to the reactant molecules. It should be pointed out that these very small Au–Cu alloy particles were obtained by a high-temperature treatment, *i.e.*, 500 °C-calcination in air and 550 °C-reduction in H_2, demonstrating that they are very stable and highly resistant to sintering.

Such highly dispersed Au–Cu alloy particles are expected to find wide applications in catalysis. In the present work, we choose CO oxidation as a probe reaction to demonstrate the synergy between gold and copper. Fig. 4(a) shows the CO conversions as a function of reaction temperatures. The Cu/SBA-15 was inactive below 100 °C, but the Au/SBA-15 possessed a moderate activity at low temperatures. Interestingly, when gold was alloyed with copper, the activity was enhanced greatly. The Au–Cu/SBA-15 catalysts were already active even below 0 °C, and the CO conversion increased with the reaction temperature and it reached 100% at 25 °C. To compare the intrinsic activity of our Au–Cu/SBA-15 with those of Au/SiO_2 in the literature, we calculated the specific reaction rate, the contact time, as well as the turnover frequencies (TOFs), as listed in Table 1. It can be seen that the Au–Cu(1/1)/SBA-15 gave a specific reaction rate of 0.43 $mol_{CO}\ g_{Au}^{-1}\ h^{-1}$ at 20 °C at a very short contact time, while the Au/SiO_2, which was reported by Budroni and Corma *et al.*[16] to have a comparable activity with Au/TiO_2, gave a specific reaction rate of 0.48 $mol_{CO}\ g_{Au}^{-1}\ h^{-1}$ at 30 °C at a contact time at least one order of magnitude longer than that in our case. Evidently, our Au–Cu(1/1)/SBA-15 possessed the higher activity, with the TOF three times as large as that on the Au/MCM-41 prepared by CVD.[20] Moreover, it is noted that the Au–Cu(1/1)/SBA-15 was more active than the Au–Cu(3/1)/SBA-15 although they had almost the same particle size. This result implies that the enhanced activity of gold by alloying with copper cannot only be attributed to the decreased particle size. The presence of copper with an intimate contact with gold, we believe, would also modify the electronic properties of gold, and thereby contribute much to the activation of oxygen. In other words, the synergy between gold and copper in catalyzing CO oxidation can be ascribed to both the geometric and the electronic effects.

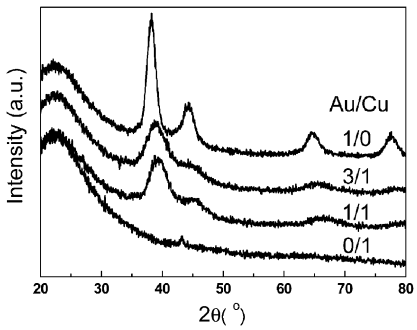

Fig. 1 XRD Patterns of Au–Cu/SBA-15 with different Au : Cu atomic ratios.

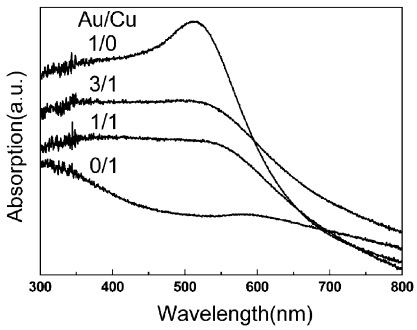

Fig. 2 UV-Vis spectra of Au–Cu/SBA-15 with different Au : Cu atomic ratios.

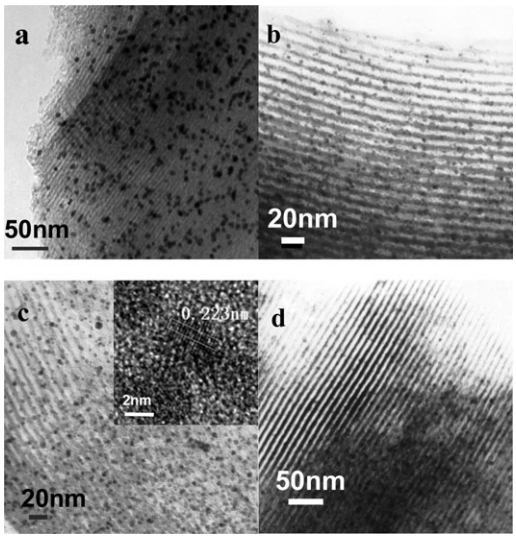

Fig. 3 TEM images of Au–Cu/SBA-15 with (a) Au : Cu = 1 : 0; (b) Au : Cu = 3 : 1; (c) Au : Cu = 1 : 1 and (d) Au : Cu = 0 : 1.

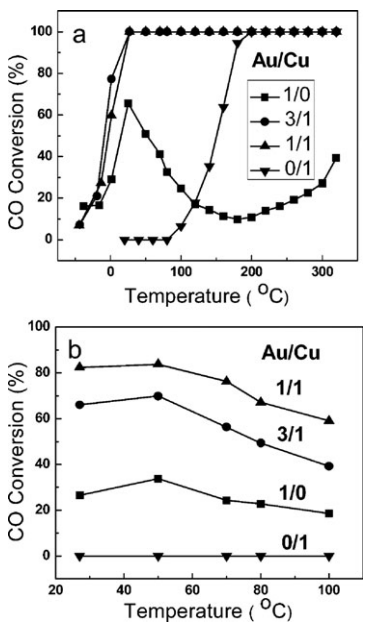

Fig. 4 CO conversions with reaction temperature over Au–Cu/SBA-15: (a) CO–O_2–He = 1 : 1 : 98, GHSV = 20 000 ml g_{cat}^{-1} h^{-1}; (b) CO–O_2–H_2–He = 1 : 0.5 : 50 : 48.5, GHSV = 40 000 ml g_{cat}^{-1} h^{-1}.

When a large amount of H_2 was present in the reaction stream, our Au–Cu alloy system was also very active and selective for the preferential oxidation of CO, as shown in Fig. 4(b). Although the CO conversion decreased with the reaction temperature due to competitive oxidation of hydrogen, it still attained a value 67.1% for Au : Cu = 1 : 1 and 49.3% for Au : Cu = 3 : 1 at the reaction temperature of 80 °C, which is the operational temperature for a fuel cell. A further stability test with the presence of 20% CO_2 showed that the CO conversion on the Au–Cu (1/1)/SBA-15 remained at 57% over a 25 h run at 80 °C, demonstrating the catalyst is stable and has a good tolerance to CO_2 (Fig. S1, ESI†). We must emphasize that the present Au–Cu alloy system is superior to our previously developed Au–Ag alloy system in the preferential oxidation of CO, because the latter system was deactivated completely by the rich presence of H_2.[17]

In conclusion, we for the first time synthesized Au–Cu alloy nanoparticles which are highly dispersed in the channels of the SBA-15 support and are highly resistant to sintering even after high temperature treatment. This gold–copper alloy nanocatalyst is highly active for CO oxidation, even with the rich presence of hydrogen. The synergistic effect between Au and Cu we observed in CO oxidation is expected to find wide applications in other gold-involved oxidation reactions, especially in selective oxidations under mild conditions. This will merit to be further explored in the future.

Supports from the National Science Foundation of China (NSFC) (No. 20673116, 20773124) are gratefully acknowledged.

Notes and references

1. M. Haruta, T. Kobayashi, H. Sano and N. Yamada, *Chem. Lett.*, 1987, **4**, 405.
2. E. Sacaliuc, A. M. Beale, B. M. Weckhuysen and T. A. Nijhuis, *J. Catal.*, 2007, **248**, 235.
3. G. Li, J. Edwards, A. F. Carley and G. J. Hutchings, *Catal. Today*, 2006, **114**, 369.
4. M. D. Hughes, Y. J. Xu, P. Jenkins, P. McMorn, P. Landon, D. I. Enache, A. F. Carley, G. A. Attard, G. J. Hutchings, F. King, E. H. Stitt, P. Johnston, K. Griffin and G. J. Kiely, *Nature*, 2005, **437**, 1132.
5. C. González-Arellano, A. Corma, M. Iglesias and F. Sánchez, *J. Catal.*, 2006, **238**, 497.
6. X. K. Wang, A. Q. Wang, X. D. Wang, X. F. Yang and T. Zhang, *Gold Bull.*, 2007, **40**, 52.
7. A. Corma and P. Serna, *Science*, 2006, **313**, 332.
8. Y. Segura, N. López and J. Pérez-Ramírez, *J. Catal.*, 2007, **247**, 383.
9. G. C. Bond and D. T. Thompson, *Catal. Rev. Sci. Eng.*, 1999, **41**, 319.
10. M. M. Schubert, S. Hackenberg, A. C. Veen, M. Muhler, V. Plzak and R. J. Behm, *J. Catal.*, 2001, **197**, 113.
11. M. Daté, M. Okumura, S. Tsubota and M. Haruta, *Angew. Chem., Int. Ed.*, 2004, **43**, 2129.
12. M. S. Chen and D. W. Goodman, *Science*, 2004, **306**, 252.
13. M. Mihaylov, E. Ivanova, Y. Hao, K. Hadjiivanov, B. C. Gates and H. Knözinger, *Chem. Commun.*, 2008, 175.
14. M. Comotti, W. C. Li, B. Spliethoff and F. Schüth, *J. Am. Chem. Soc.*, 2006, **128**, 917; W. C. Li, M. Comotti, A. H. Lu and F. Schüth, *Chem. Commun.*, 2006, 1772.
15. W. Yan, S. M. Mahurin, B. Chen, S. H. Overbury and S. Dai, *J. Phys. Chem. B*, 2005, **109**, 15489.
16. G. Budroni and A. Corma, *Angew. Chem., Int. Ed.*, 2006, **45**, 3328.
17. J. H. Liu, A. Q. Wang, Y. S. Chi, H. P. Lin and C. Y. Mou, *J. Phys. Chem. B*, 2004, **109**, 40; A. Q. Wang, J. H. Liu, S. D. Lin, T. S. Lin and C. Y. Mou, *J. Catal.*, 2005, **233**, 186; A. Q. Wang, Y. P. Hsieh, Y. F. Chen and C. Y. Mou, *J. Catal.*, 2006, **237**, 197; A. Q. Wang, C. M. Chang and C. Y. Mou, *J. Phys. Chem. B*, 2005, **109**, 18860.
18. C. H. Tu, A. Q. Wang, M. Y. Zheng, X. D. Wang and T. Zhang, *Appl. Catal., A*, 2006, **297**, 40.
19. S. Pal and G. De, *J. Mater. Chem.*, 2007, **17**, 493.
20. M. Okumura, S. Nakamura, S. Tsubota, T. Nakamura, M. Azuma and M. Hartua, *Catal. Lett.*, 1998, **51**, 53.